GEOGRAPHICAL REPORTS
OF TOKYO METROPOLITAN UNIVERSITY 59 (2024) 135–142

MAJOR ELEMENT COMPOSITION OF VOLCANIC GLASS SHARDS IN LATE QUATERNARY TEPHRAS FROM THE TOWADA VOLCANO, NORTHEAST JAPAN

Daisuke ISHIMURA

Abstract The Towada volcano, a prominent active volcano in the Tohoku region, has played a crucial role in providing widespread tephras. These tephras, beyond shaping the local geomorphology and geology, hold increasing significance as they are discovered in sediments of distal regions with the importance of climate change studies. The major element composition of volcanic glass shards, constituting the tephra, serves as a vital indicator for identifying these layers far from the source volcano. This study comprehensively measures the chemical compositions of major tephras of the Towada volcano from the late Quaternary to the present. While the chemical composition of each tephra exhibits similarities, distinctive characteristics are evident. Notably, SiO_2 values in the Holocene show an increasing trend from older to more recent eruptive events, suggesting a shift toward more felsic tephras. In the Pleistocene, though less pronounced, variations and challenges in identification persist, emphasizing the importance of considering multiple information, such as stratigraphy, volcanic glass morphology, refractive index, mineral composition, and other chronological markers.

Keywords: volcanic glass, Towada volcano, major element composition, Holocene, Pleistocene

1. Introduction

The Towada volcano, situated in the northern part of northeast Japan (Fig. 1), commenced activity around 220 ka (Kudo *et al*. 2019). Its volcanic history unfolds in three phases: precaldera (220–61 ka), caldera-forming (61–15.5 ka), and postcaldera (15.5 ka to the present) (Hayakawa 1985; Kudo *et al.* 2019). Throughout these periods, substantial tephra emissions covered extensive areas and have been identified as widespread tephras (Machida and Arai 2003). Recent discoveries in the varve sediments of Lake Suigetsu (McLean *et al*. 2018) and international identifications (Bourne *et al*. 2016; Sun *et al*. 2021) emphasize the global significance of these tephras beyond their role as age markers. However, the similarities in characteristics among tephras from a single volcano necessitate a comprehensive analysis and comparison for proper identification and differentiation. This study focuses on the major element compositions of volcanic glass shards in late Quaternary tephras from the Towada volcano. The samples selected have existing data on volcanic glass morphology, heavy mineral composition, and refractive index of volcanic glass shards (Table 1; Ishimura *et al.* 2014; Miyazaki and Ishimura 2018). Additionally, two uncorrelated samples from the Pacific coast of the Tohoku region were analyzed and correlated with tephras from the Towada volcano.

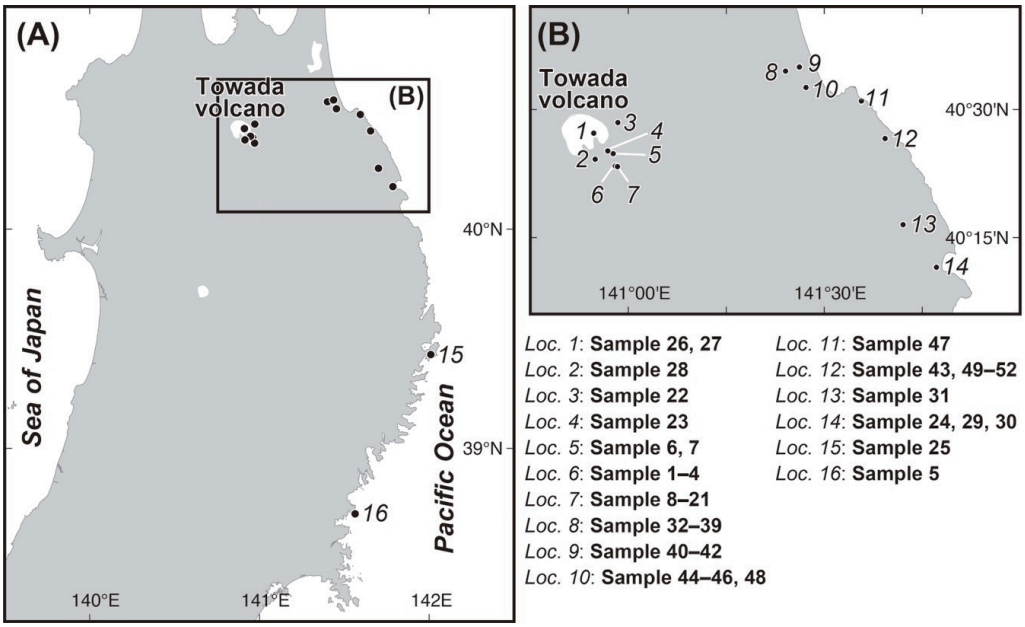

Fig. 1 Location map of sampling sites. See Table S1 (downloadable from the GR website) for more information on samples.

2. Material and Method

Tephra samples

Holocene tephras of the Towada volcano in the proximal area have been previously documented by Oike (1972) and Hayakawa (1985). A more recent and systematic analysis by Kudo and Sasaki (2007), Kudo (2008), and Kudo (2010) has detailed the tephrostratigraphy and eruption ages of these Holocene tephras. The Towada volcano's recent eruption history, categorized as episodes A to G (Hayakawa 1985), has also been extensively covered by Kudo and Sasaki (2007), Kudo (2008), and Kudo (2010). This study focuses on measuring glass geochemistry within To-a (episode A), To-b (episode B), To-Cu (episode C), Herai ash (episode D'), Oguni pumice (episode D), and To-Nb (episode E) in the Holocene period (Table 1). The chemical composition of To-Cu, consisting of Utarube ash, Kanegasawa pumice, and Chuseri pumice from the youngest to the oldest (Hayakawa 1985), has been previously reported by Ishimura and Hiramine (2020) and is used for comparison with other Holocene tephras in this study. Additionally, two uncorrelated tephra samples from different outcrops were analyzed. One, labeled Sample No. 31, is a 20 cm thick tephra composed of yellow pumice lapilli, situated about 1 m below the surface at Loc. 13 (Fig. 1), within black to brown soil. The second sample, labeled Sample No. 5, is from an outcrop facing the coast at Loc. 16 (Fig. 1), where a brown volcanic ash layer is situated approximately 1.5 m below the surface, overlain by soil, talus deposits, and rounded gravel deposits. Both are considered Holocene tephras based on their depth from the surface and stratigraphy.

Given the extensive coverage of the Towada volcano's Pleistocene tephras on the marine

Table 1 Holocene and Pleistocene tephras from the Towada volcano

	Generic tephra name	Eruptive episode	Eruption product name	Age	SEM-EDS analysis
Holocene	To-a	Episode A	Kemanai pyroclastic flow deposits	AD 915*	○
			Oyu 3 pumice		○
			Oyu 2 ash		○
			Oyu 1 pumice		○
	To-b	Episode B	Soube ash	2.8 ka**	
			Mayogatai pumice		○
	To-Cu	Episode C	Utarube ash	5.9-6.0 ka***	○
			Kanegasawa pumice		○
			Chuseri pumice		○
	-	Episode D'	Herai ash	7.6 ka**	○
	-	Episode D	Nakanosawa ash	8.3 ka**	
			Oguni pumice		○
	To-Nb	Episode E	Kaimori ash	9.2 ka****	
			Nambu pumice		○

	Generic tephra name	Age	SEM-EDS analysis
Pleistocene	To-H, HP	15 ka*	○
	To-BP2	ca. 20 ka*	○
	To-Of, BP1	>32 ka*	○
	To-G	MIS 4*	○
	To-Kb	58±4 ka*****	○
	To-Os, Rd	61±4 ka*****	
	To-SP	-	
	To-Ok_2	MIS 5a*	○
	To-QP	-	
	To-T17	-	
	To-AP	MIS 5c*	○
	To-CP	111±6 ka*****	○
	NP	-	○

Names of eruptive episodes and tephras in the Holocene are from Hayakawa (1985) and Kudo (2010). Tephra names in the Late Pleistocene are from Machida and Arai (2003). *: Machida and Arai (2003), **: Kudo and Sasaki (2007), ***: McLean *et al*. (2018), ****: Kudo (2008), *****: Ito *et al*. (2017).

terraces in the Kamikita Plain (Koike and Machida 2001), studies on these tephras have evolved in tandem with chronological investigations of the terraces (Table 1; Tohoku Region Quaternary Research Group 1969; Oike *et al*. 1970; Miyauchi 1985; Kuwabara 2010). Petrological characteristics of the Pleistocene tephras in the Kamikita Plain have been elucidated (Machida and Arai 2003; Kuwabara 2010). Ito *et al*. (2017) conducted optical stimulated luminescence dating of sediments covering marine terraces, providing age estimates for the Towada volcano tephras (Table 1). For Pleistocene tephras, this study measured To-H, To-HP, To-BP2, To-Of, To-G, To-Kb, To-Ok_2, To-AP, To-CP, and NP tephras. Chemical compositions of NP, To-CP, To-AP, and To-Ok_2 were previously reported by Miyazaki and Ishimura (2018) and are included in this study for comparative analysis with other Pleistocene tephras. However, chemical compositions for other tephras, though information on the refractive index of volcanic glass shards and heavy mineral composition is available (Miyazaki and Ishimura 2018), were not previously measured. This study fills that gap by measuring the chemical compositions of To-H, To-HP, To-BP2, To-Of, To-G, and To-Kb tephras. Sample locations are depicted in Figure 1, and detailed sample information, including tephra names, coordinates, and references, is available in Table S1 (downloadable from the GR website).

SEM-EDS analysis

The tephra analysis utilized the 62–120 μm fractions, previously rinsed and sieved as outlined in prior studies. From December 2016 to July 2021, an energy dispersive X-ray spectrometer (EDAX GENESIS APEX2 and JEOL JSM-6930) was employed to measure the major element composition of volcanic glass shards, following the method and analysis conditions detailed by Suzuki *et al*. (2014). Volcanic glass shards of Aira-Tn tephra (AT) (Machida and Arai 2003) were used as a working standard for assessing data reproducibility and instrument stability. Chemical compositions reported in Miyazaki and Ishimura (2018) and Ishimura and Hiramine (2020) were measured using the same instruments and procedures applied in this study.

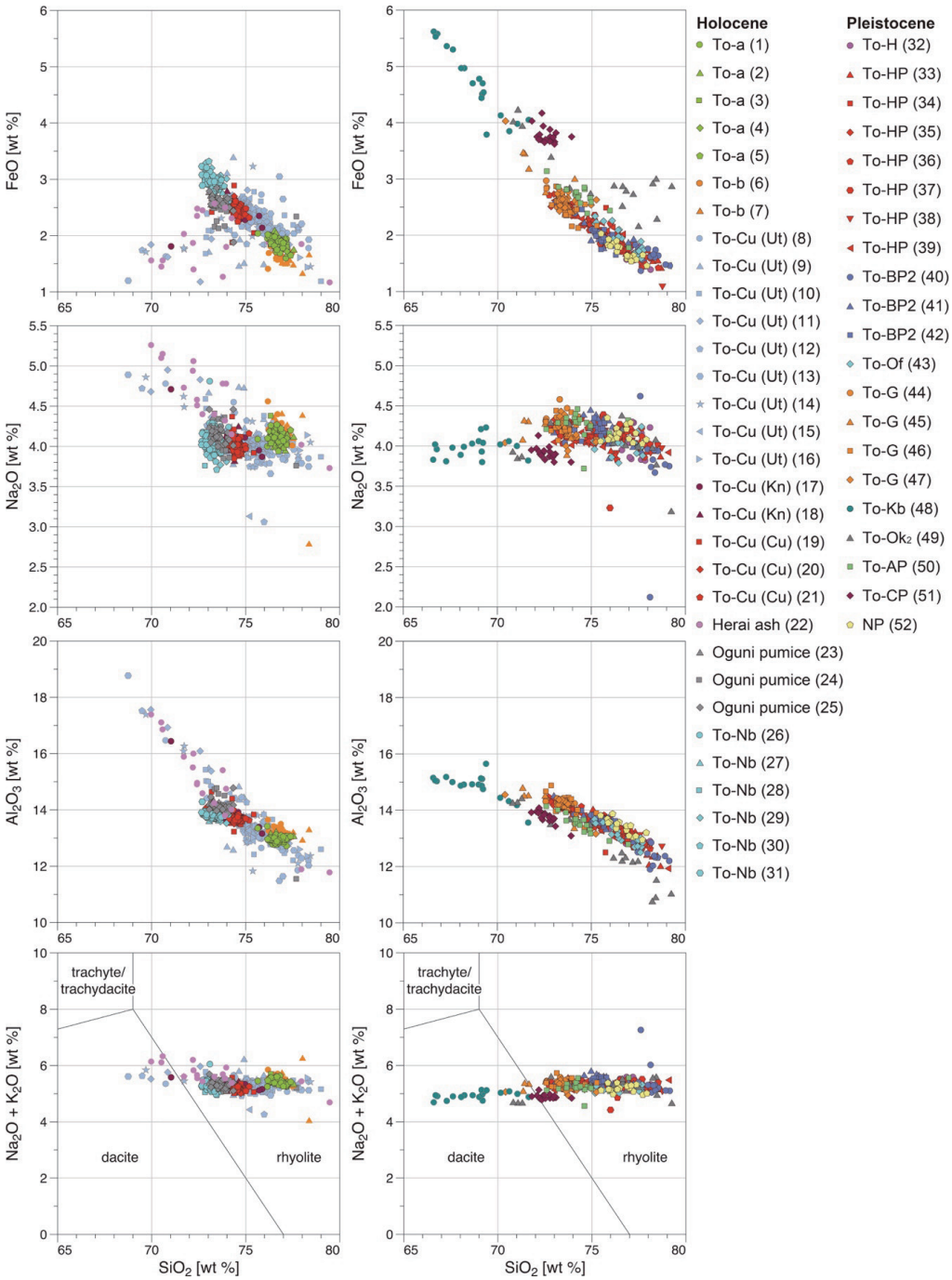

Fig. 2 Characteristics of the major element composition of volcanic glass shards. Rock types are classified based on Le Bas *et al.* (1986).

Table 2 Mean and standard deviation of the major element composition

	SiO_2	TiO_2	Al_2O_3	FeO*	MnO	MgO	CaO	K_2O	Na_2O	Total**
Sample No. 1	76.7	0.4	13.0	1.9	0.1	0.5	2.0	1.3	4.1	97.9
To-a (Kemanai pyroclastic flow deposits)	0.4	0.1	0.2	0.1	0.1	0.0	0.1	0.1	0.0	0.8
Sample No.2	76.7	0.4	13.0	1.9	0.1	0.5	2.0	1.3	4.1	97.9
To-a (Oyu3 pumice)	0.4	0.1	0.1	0.1	0.1	0.1	0.1	0.1	0.1	0.7
Sample No. 3	76.7	0.4	12.9	1.9	0.1	0.5	2.0	1.3	4.1	97.7
To-a (Oyu2 ash)	0.3	0.1	0.1	0.1	0.1	0.0	0.1	0.0	0.1	0.9
Sample No. 4	76.7	0.4	12.9	1.9	0.1	0.5	2.1	1.3	4.1	97.7
To-a (Oyu1 pumice)	0.2	0.1	0.1	0.1	0.1	0.0	0.1	0.1	0.1	1.1
Sample No. 5	76.7	0.4	13.0	1.8	0.1	0.5	2.0	1.3	4.1	97.6
To-a	0.3	0.1	0.1	0.1	0.1	0.0	0.1	0.1	0.1	0.6
Sample No. 6	76.7	0.3	13.3	1.7	0.1	0.5	2.0	1.3	4.2	97.8
To-b (Mayogatai pumice)	0.3	0.1	0.2	0.1	0.1	0.1	0.1	0.1	0.1	1.2
Sample No. 7	77.1	0.3	13.1	1.6	0.1	0.5	1.9	1.3	4.1	98.3
To-b (Mayogatai pumice)	0.5	0.1	0.1	0.1	0.1	0.1	0.2	0.1	0.4	0.6
Sample No. 8	75.7	0.5	13.2	2.2	0.1	0.5	2.3	1.3	4.1	97.1
To-Cu (Utarube ash)	1.6	0.1	0.9	0.2	0.1	0.1	0.7	0.2	0.2	1.5
Sample No. 9	75.2	0.5	13.5	2.3	0.2	0.6	2.5	1.3	4.1	97.7
To-Cu (Utarube ash)	0.8	0.1	0.7	0.5	0.1	0.3	0.3	0.1	0.3	1.3
Sample No. 10	75.6	0.5	13.3	2.2	0.1	0.5	2.3	1.3	4.1	97.2
To-Cu (Utarube ash)	1.4	0.1	0.8	0.4	0.1	0.2	0.5	0.1	0.2	1.8
Sample No. 11	74.7	0.4	13.9	2.2	0.1	0.6	2.7	1.2	4.1	97.7
To-Cu (Utarube ash)	1.8	0.1	1.4	0.4	0.1	0.2	0.7	0.2	0.3	1.0
Sample No. 12	75.1	0.4	13.7	2.3	0.1	0.7	2.6	1.2	4.0	97.9
To-Cu (Utarube ash)	1.6	0.1	1.0	0.2	0.1	0.2	0.6	0.1	0.3	0.9
Sample No. 13	76.0	0.5	13.1	2.2	0.1	0.5	2.3	1.3	4.0	96.9
To-Cu (Utarube ash)	2.0	0.1	1.5	0.4	0.1	0.2	0.7	0.1	0.3	1.2
Sample No. 14	74.8	0.5	13.7	2.3	0.2	0.6	2.6	1.2	4.1	98.0
To-Cu (Utarube ash)	1.9	0.1	1.4	0.4	0.1	0.2	0.7	0.1	0.3	0.9
Sample No. 15	75.2	0.5	13.5	2.4	0.2	0.6	2.5	1.2	4.0	97.2
To-Cu (Utarube ash)	0.8	0.1	0.4	0.3	0.1	0.1	0.2	0.1	0.2	1.3
Sample No. 16	75.3	0.5	13.4	2.3	0.1	0.6	2.5	1.2	4.0	98.3
To-Cu (Utarube ash)	1.1	0.1	0.4	0.3	0.1	0.1	0.3	0.1	0.1	1.2
Sample No. 17	74.6	0.5	13.8	2.4	0.2	0.7	2.7	1.2	4.1	98.7
To-Cu (Kanegasawa pumice)	0.9	0.1	0.6	0.2	0.1	0.1	0.3	0.1	0.2	0.4
Sample No. 18	74.5	0.5	13.7	2.5	0.2	0.7	2.7	1.2	4.0	98.8
To-Cu (Kanegasawa pumice)	0.2	0.0	0.1	0.1	0.1	0.0	0.1	0.1	0.1	1.2
Sample No. 19	74.5	0.5	13.7	2.5	0.2	0.7	2.7	1.2	4.0	98.3
To-Cu (Chuseri pumice)	0.4	0.1	0.3	0.2	0.1	0.1	0.1	0.1	0.1	1.4
Sample No. 20	74.4	0.5	13.7	2.5	0.2	0.7	2.8	1.2	4.0	98.9
To-Cu (Chuseri pumice)	0.4	0.1	0.1	0.1	0.1	0.1	0.1	0.1	0.1	1.5
Sample No. 21	74.5	0.5	13.7	2.4	0.2	0.7	2.8	1.2	4.0	98.1
To-Cu (Chuseri pumice)	0.3	0.1	0.1	0.1	0.1	0.1	0.1	0.1	0.1	1.4
Sample No. 22	73.4	0.5	14.8	1.9	0.1	0.4	3.2	1.1	4.6	97.5
Herai ash	2.5	0.2	1.6	0.5	0.1	0.1	0.6	0.2	0.4	1.8
Sample No. 23	73.3	0.6	14.2	2.6	0.2	0.8	3.0	1.2	4.2	98.1
Oguni pumice	0.2	0.1	0.1	0.1	0.0	0.0	0.0	0.0	0.1	0.8
Sample No. 24	74.0	0.5	14.1	2.5	0.2	0.7	2.8	1.2	4.1	98.3
Oguni pumice	1.0	0.1	0.7	0.2	0.1	0.1	0.4	0.1	0.2	1.0
Sample No. 25	73.7	0.5	14.1	2.6	0.2	0.7	2.9	1.2	4.2	98.1
Oguni pumice	0.4	0.1	0.2	0.2	0.1	0.1	0.1	0.1	0.1	1.4
Sample No. 26	73.3	0.6	13.8	2.9	0.2	0.8	3.0	1.2	4.3	98.4
To-Nb	0.3	0.1	0.1	0.1	0.1	0.0	0.1	0.1	0.2	1.1
Sample No. 27	73.4	0.6	13.7	2.9	0.2	0.8	3.0	1.3	4.2	95.7
To-Nb	0.2	0.1	0.1	0.1	0.1	0.0	0.1	0.0	0.1	1.5
Sample No. 28	73.0	0.6	13.9	3.0	0.2	0.8	3.2	1.3	4.0	98.6
To-Nb	0.2	0.1	0.1	0.1	0.1	0.0	0.1	0.0	0.1	0.8
Sample No. 29	73.4	0.6	13.8	3.0	0.2	0.8	3.0	1.3	4.0	98.2
To-Nb	0.3	0.1	0.1	0.1	0.0	0.0	0.1	0.1	0.1	0.5
Sample No. 30	73.3	0.6	13.9	3.0	0.2	0.8	3.1	1.2	4.0	97.4
To-Nb	0.3	0.1	0.1	0.1	0.1	0.0	0.1	0.1	0.1	1.8
Sample No. 31	73.0	0.6	13.9	3.1	0.2	0.8	3.2	1.2	4.0	98.7
To-Nb	0.2	0.1	0.1	0.1	0.1	0.1	0.1	0.0	0.1	0.4

	SiO_2	TiO_2	Al_2O_3	FeO*	MnO	MgO	CaO	K_2O	Na_2O	Total**
Sample No. 32	77.1	0.3	13.0	1.7	0.1	0.5	2.0	1.2	4.1	95.3
To-H	0.7	0.1	0.2	0.2	0.1	0.1	0.1	0.1	0.2	1.5
Sample No. 33	76.4	0.4	13.2	1.9	0.1	0.6	2.2	1.2	4.1	95.4
To-HP	1.7	0.1	0.7	0.3	0.1	0.1	0.4	0.1	0.1	1.5
Sample No. 34	75.6	0.4	13.4	2.0	0.2	0.6	2.4	1.2	4.2	96.6
To-HP	1.3	0.1	0.5	0.3	0.1	0.1	0.3	0.1	0.1	1.1
Sample No. 35	73.9	0.5	14.0	2.4	0.1	0.8	2.9	1.1	4.2	98.1
To-HP	1.0	0.1	0.3	0.3	0.1	0.1	0.3	0.1	0.1	0.6
Sample No. 36	75.2	0.4	13.6	2.2	0.1	0.7	2.5	1.2	4.1	96.6
To-HP	1.9	0.2	0.7	0.5	0.1	0.2	0.5	0.1	0.1	1.6
Sample No. 37	76.3	0.4	13.3	1.8	0.1	0.6	2.3	1.2	4.1	96.6
To-HP	0.8	0.1	0.3	0.2	0.1	0.1	0.2	0.1	0.2	1.6
Sample No. 38	76.0	0.3	13.4	1.9	0.1	0.6	2.3	1.2	4.1	95.9
To-HP	1.3	0.2	0.4	0.3	0.1	0.1	0.3	0.1	0.1	1.8
Sample No. 39	75.5	0.4	13.5	2.1	0.2	0.6	2.4	1.2	4.1	97.1
To-HP	1.4	0.1	0.6	0.3	0.1	0.1	0.4	0.1	0.1	1.6
Sample No. 40	77.2	0.4	12.8	1.8	0.1	0.5	1.8	1.5	3.9	94.3
To-BP2	1.7	0.1	0.7	0.3	0.1	0.1	0.6	0.7	0.5	2.0
Sample No. 41	75.6	0.4	13.6	2.0	0.1	0.6	2.3	1.3	4.2	95.8
To-BP2	0.9	0.1	0.3	0.2	0.1	0.1	0.2	0.1	0.2	2.0
Sample No. 42	75.5	0.4	13.6	2.0	0.1	0.6	2.4	1.2	4.2	95.5
To-BP2	0.4	0.1	0.1	0.2	0.1	0.0	0.1	0.1	0.1	1.7
Sample No. 43	76.6	0.4	13.1	2.0	0.1	0.5	2.2	1.2	4.0	94.2
To-Of	0.9	0.1	0.3	0.2	0.1	0.1	0.2	0.1	0.1	1.4
Sample No. 44	73.4	0.5	14.2	2.6	0.2	0.8	2.9	1.0	4.3	97.5
To-G	0.4	0.1	0.2	0.1	0.1	0.0	0.1	0.1	0.1	1.2
Sample No. 45	73.2	0.6	14.3	2.7	0.2	0.9	2.9	1.1	4.2	95.3
To-G	0.9	0.1	0.3	0.3	0.1	0.1	0.3	0.1	0.1	2.1
Sample No. 46	73.7	0.5	14.2	2.5	0.2	0.8	2.8	1.1	4.2	97.7
To-G	0.6	0.1	0.3	0.2	0.1	0.1	0.2	0.1	0.1	1.0
Sample No. 47	73.5	0.5	14.1	2.7	0.2	0.8	2.8	1.0	4.2	96.0
To-G	1.0	0.1	0.4	0.3	0.1	0.1	0.3	0.1	0.1	2.0
Sample No. 48	68.8	0.8	14.8	4.7	0.2	1.5	4.2	1.0	4.0	98.6
To-Kb	1.5	0.1	0.5	0.6	0.1	0.3	0.4	0.1	0.1	0.6
Sample No. 49	75.6	0.7	12.6	3.0	0.1	0.5	2.2	1.2	4.0	96.1
To-Ok_2	2.8	0.1	1.2	0.6	0.1	0.4	0.9	0.2	0.3	2.3
Sample No. 50	74.4	0.6	13.5	2.7	0.2	0.7	2.7	1.0	4.3	97.1
To-AP	1.0	0.1	0.4	0.3	0.0	0.1	0.3	0.1	0.2	1.5
Sample No. 51	72.6	0.7	13.7	3.8	0.2	0.9	3.2	1.0	3.9	98.6
To-CP	0.5	0.1	0.2	0.1	0.1	0.1	0.2	0.0	0.1	0.7
Sample No. 52	76.6	0.3	13.4	1.7	0.2	0.5	2.1	1.0	4.1	93.3
NP	0.7	0.1	0.3	0.2	0.1	0.1	0.2	0.1	0.1	1.3
Working standard	77.9	0.1	12.5	1.3	0.1	0.2	1.1	3.2	3.5	95.4
AT	0.3	0.1	0.1	0.1	0.1	0.0	0.1	0.1	0.1	1.4

Number on the upper line is the mean value and that on the lower line is the standard deviation. Measured values were recalculated to 100% on a water-free basis. *: Total iron oxide as FeO. **: raw data before recalculations to 100 % on a water-free basis.

3. Result and Discussion

The dataset, inclusive of individual data, mean values, and standard deviations for the major element composition of individual volcanic glass shards determined via SEM-EDS analysis, is presented in Table 2 and S2 (downloadable from the GR website). Diagrams illustrating SiO_2–FeO, SiO_2–Na2O, SiO_2–Al_2O_3, and SiO_2–Na_2O + K_2O relationships are shown in Fig. 2.

Holocene tephras (To-a~To-Nb)

Except for the Herai and Utarube ashes, the Towada volcano's Holocene tephras are predominantly rhyolitic (SiO_2–Na_2O + K_2O in Fig. 2) and exhibit distinct, individually identifiable patterns (Fig. 2).

The To-Nb tephra shows one of the lowest SiO_2 content (72.7–74.1 wt%) among the Holocene

tephras. Positioned between the To-Nb and To-Cu tephras, the Oguni pumice exhibits SiO_2 values of 73.1–77.7 wt%, FeO values of 1.9–2.9 wt%, and slightly higher Al_2O_3 (11.6–14.8 wt%) than the To-Nb and To-Cu tephras. The Herai ash demonstrates SiO_2 ranging from 70.0–79.5 wt%. The To-Cu tephra presents similar chemical compositions for Kanegasawa and Chuseri pumice, differing from Utarube ash. Kanegasawa and Chuseri pumice exhibit SiO_2 values of 71.0–75.9 wt% and FeO values of 1.8–2.9 wt%. Utarube ash, while variable, predominantly features higher SiO_2 values than Kanegasawa and Chuseri pumice. The To-b tephra shows one of the highest SiO_2 contents (76.2–78.4 wt%) among Holocene tephras, similar to the To-a tephra, but with slightly lower FeO (1.3–1.9 wt%) and Al_2O_3 (12.9–13.7 wt%) than the To-a tephra. The To-a tephra, with the highest SiO_2 content (75.6–77.6 wt%) among Holocene tephras, is divided into four units in the proximal area, all exhibiting similar chemical compositions.

Based on the results of the chemical compositions, the tephra at Loc. 13 (Sample No. 31) is correlated with To-Nb, and the tephra at Loc. 16 (Sample No. 5) is correlated with To-a. Both tephras are expected to be fallout tephras at the outcrop sites according to existing studies (e.g., Machida and Arai 2003). The recent identification of Oguni pumice at distal sites by Ishimura *et al*. (2014) is supported by chemical composition analyses. Holocene tephra data reveal a gradual increase in SiO_2 values from To-Nb to To-a.

Pleistocene tephras (To-H~NP)

The Towada volcano's Pleistocene tephras exhibit dacitic composition in the To-Kb tephra, dacitic to rhyolitic composition in the To-Ok_2 and To-CP tephras, and are predominantly rhyolitic in the rest, as indicated by the SiO_2–$Na_2O + K_2O$ relationship in Fig. 2. In contrast to Holocene tephras, the Pleistocene counterparts show significant SiO_2 variation even within single tephra. Individual characteristics of these Pleistocene tephras are detailed below.

The NP tephra shows one of the highest SiO_2 contents in the Pleistocene, ranging from 75.5 to 77.9 wt%. This tephra exhibits low FeO (1.5–2.0 wt%) and high Al_2O_3 (13.0–13.9 wt%) compared to other Pleistocene Towada tephras, aligning closely with the characteristics of the To-H and To-Of tephras discussed below. The To-CP tephra stands out among Pleistocene tephras, positioned in the dacitic to rhyolitic range. Notably, it showcases high FeO (3.6–4.2 wt%) and low Na_2O (3.8–4.1 wt%). The To-AP tephra shares similarities with the To-G tephra but features slightly higher FeO (1.8–3.1 wt%) and lower Al_2O_3 (12.8–14.1 wt%) than the To-G tephra. Characterized by SiO_2 variation from 70.8 to 79.3 wt%, the To-Ok_2 tephra is notably diverse. The To-Kb tephra, previously mentioned as dacitic, exhibits a trend on diagrams akin to the To-CP tephra. The To-G tephra demonstrates lower SiO_2 content (70.4–75.3 wt%) than Pleistocene tephras subsequent to the To-Of tephras. However, its trend on the diagrams is similar to them. Although To-Of, To-BP2, To-HP, and To-H exhibit similar chemical compositions, To-Of (75.2–77.7 wt%) and To-H (75.6–78.1 wt%) show minimal SiO_2 variation, while To-BP2 (73.0–79.1 wt%) and To-HP (72.7–79.1 wt%) exhibit substantial SiO_2 variability.

For Pleistocene tephras beyond the To-Of tephra, chemical composition similarities make geochemistry-based correlation challenging. However, those predating To-Of can be individually identified, except for the NP tephra. Consequently, additional information such as stratigraphy, volcanic glass morphology, refractive index, heavy mineral composition, and age information is deemed necessary for a comprehensive discussion on tephras from To-Of to To-H. The significance of including hornblende as a heavy mineral in distinguishing To-H and To-Of tephras has been emphasized (Machida and Arai 2003). However, it was also noted that the To-Of tephra also contains a small amount of hornblende, and the need for more precise chemical analysis

(LA-ICP-MS) was mentioned (Furusawa 2017). Identifying Pleistocene tephras from the Towada volcano requires a holistic interpretation incorporating not only chemical compositions but also other pertinent information. Moreover, since many tephras older than the To-Ok_2 tephra have lost their volcanic glass shards due to weathering, characteristics like heavy minerals prove valuable for correlation (Miyazaki and Ishimura 2018). Comparing Holocene and Pleistocene tephras, the Pleistocene exhibits a larger variation in chemical composition. The connection of this difference to eruption style, size, or the caldera formation process warrants further examination.

4. Conclusions

This study undertook the measurement of major element compositions of volcanic glass shards in Late Pleistocene to Holocene tephras originating from the Towada volcano. The findings reveal consistent chemical composition trends across this timeframe, yet the subtle variations in values enable the identification of numerous tephras. In contrast, for those with similar compositions, reliance on additional information beyond chemical composition enhances the reliability of identification and correlation. Additionally, since this study was not able to measure samples from multiple sites for a single tephra, future analyses encompassing multiple sites and units would contribute to more robust identification and correlation.

Acknowledgments

I thank Dr. Reona Hiramine (Tokyo Metropolitan University) for illustrating Figures 1 and 2.

References

Bourne, A. J., Abbott, P. M., Albert, P. G., Cook, E., Pearce, N. J. G., Ponomareva, V., Svensson, A. and Davies, S. M. 2016. Underestimated risks of recurrent long-range ash dispersal from northern Pacific Arc volcanoes. *Scientific Reports* **6**: 29837. DOI: 10.1038/srep29837.

Hayakawa, Y. 1985. Pyroclastic geology of Towada volcano. *Bulletin of the Earthquake Research Institute, University of Tokyo* **60**: 507–592.

Furusawa, A. 2017. Geochemical discrimination of individual glass shards from Towada-Ofudo and Towada-Hachinohe tephras using their trace element compositions determined by laser ablation ICP-MS. *The Journal of the Geological Society of Japan* **123**: 765–776.**

Koike, K. and Machida, H. 2001. *Construction of Quaternary Marine Terrace Atlas*. University of Tokyo Press.*

Kudo, T. 2008. Radiocarbon ages of the eruptive products from the eruptive episodes E and G, Towada volcano, northeast Japan. *Bulletin of the Volcanological Society of Japan* **53**: 193–199.**

Kudo, T. 2010. Eruption age and sequence of Ogurayama lava dome at Towada volcano, northeast Japan arc. *Bulletin of the Volcanological Society of Japan* **55**: 89–107.**

Kudo, T. and Sasaki, H. 2007. High-precision chronology of eruptive products during the post-caldera stage of Towada volcano, northeast Japan. *Journal of Geography (Chigaku Zasshi)* **116**: 653–663.**

Kudo, T., Uchino, T. and Hamasaki, S. 2019. *Geology of the Towada Ko District. Quadrangle Series, 1:50,000*. Geological Survey of Japan, AIST.*

Kuwabara, T. 2010. Tephrostratigraphy of late Middle Pleistocene to Holocene eolian deposits in drill cores recovered from the Kamikita Plain, Northeast Japan. *Bulletin of the Geological Survey of Japan* **61**: 489–494.*

Ishimura, D., Yamada, K., Miyauchi, T. and Hayase, R. 2014. Characteristics of tephras interbedded with the Holocene sediments on the Sanriku Coast, northeast Japan. *Journal of Geography (Chigaku Zasshi)* **123**: 671–697.**

Ishimura, D. and Hiramine, R. 2020. Proximal–distal fall deposit correlation of VEI-5 tephra (Towada-Chuseri) from Towada volcano, northeast Japan. *Journal of Quaternary Science* **35**: 334–348.

Ito, K., Tamura, T., Kudo, T. and Tsukamoto, S. 2017. Optically stimulated luminescence dating of Late Pleistocene tephric loess intercalated with Towada tephra layers in northeastern Japan. *Quaternary International* **456**: 154–162. DOI: 10.1016/j.quaint.2017.06.070

Le Bas, M. J., Le Maitre, R. W., Streckeisen, A. and Zanettin, B. 1986. A chemical classification of volcanic rocks based on the total alkali–silica diagram. *Journal of Petrology* **27**: 745–750.

Machida, H. and Arai, F. 2003. *Atlas of tephra in and around Japan [revised edition]*. Tokyo University Press.*

McLean, D., Albert, P. G., Nakagawa, T., Suzuki, T., Staff, R. A., Yamada, K., Kitaba, I., Haraguchi, T., Kitagawa, J., SG14 Project Members and Smith, V. 2018. Integrating the Holocene tephrostratigraphy for East Asia using a high-resolution cryptotephra study from Lake Suigetsu (SG14 core), central Japan. *Quaternary Science Reviews* **183**: 36–58. DOI: 10.1016/j.quascirev.2017.12.013

Miyauchi, T. 1985. Quaternary crustal movements estimated from deformed terraces and geologic structures of the Kamikita coastal plain, northeast Japan. *Geographical Review of Japan, Series A* **58**: 492–515.**

Miyazaki, M. and Ishimura, D. 2018. Re-examination of the ages of the last interglacial marine terraces and crustal movements since the last interglacial period along the northern Sanriku Coast based on tephrochronology. *Journal of Geography (Chigaku Zasshi)* **127**: 735–757.**

Oike, S., Matsuyama, T. and Nanasaki, O. 1970. *Report of Geological Survey in Hachinohe Plain Region (Hachinohe Heigen Chiiki Chishitsu Chosa Hokokusho)*. Tohoku Regional Agricultural Administration Offices 1–50.*

Oike, S. 1972. Holocene tephrochronology in the eastern foot-hills of the Towada volcano, northeastern Honshu, Japan. *The Quaternary Research (Daiyonki-Kenkyu)* **11**: 228–235.**

Sun, C., Plunkett, G., Zhu, Z., Zhang, L., Zhang, B., Zhang, D., Mao, Q., You, H., Wang, L., Chu, G. and Liu, J. 2021. ~5.9 cal ka bp Towada-Chuseri tephra from Towada volcano: a mid-Holocene marker layer from Japan to northeast China. *Journal of Quaternary Science* **36**: 1143–1148. DOI: 10.1002/jqs.3362

Suzuki, T., Kasahara, A., Nishizawa, F. and Saito, H. 2014. Chemical characterization of volcanic glass shards by energy dispersive X-ray spectrometry with EDAX Genesis APEX2 and JEOL JSM-6390. *Geographical reports of Tokyo Metropolitan University* **49**: 1–12.

Tohoku Region Quaternary Research Group 1969. Quaternary changes on the sea level in the Tohoku region, Japan. *Chidanken Senpo* **15**: 37–83.**

(*: in Japanese, **: in Japanese with English abstract)